AGU PUBLICATIONS

Geophysical Research Letters

RESEARCH LETTER
10.1002/2015GL067610

Key Points:
- A huge set of receiver functions is used to define a lithospheric fault at the Ionian slab edge
- The fault decouples the deformation of Apennines (delamination) from Calabrian forearc (retreat)
- The fault segments the normal fault system within the 60 km long Pollino seismic gap

Supporting Information:
- Supporting Information S1
- Figure S1

Correspondence to:
C. Chiarabba,
chiarabba@ingv.it

Citation:
Chiarabba, C., N. P. Agostinetti, and I. Bianchi (2016), Lithospheric fault and kinematic decoupling of the Apennines system across the Pollino range, *Geophys. Res. Lett.*, *43*, 3201–3207, doi:10.1002/2015GL067610.

Received 29 DEC 2015
Accepted 1 MAR 2016
Accepted article online 8 MAR 2016
Published online 13 APR 2016

Lithospheric fault and kinematic decoupling of the Apennines system across the Pollino range

Claudio Chiarabba[1], Nicola Piana Agostinetti[2], and Irene Bianchi[3]

[1]Istituto Nazionale di Geofisica e Vulcanologia, Rome, Italy, [2]Geophysics Section, School of Cosmic Physics, Dublin Institute for Advanced Studies, Dublin, Ireland, [3]Department of Meteorology and Geophysics, University of Vienna, Vienna, Austria

Abstract A persistent seismic gap is hypothesized in the Pollino area (southern Italy), at the boundary between the Apennines and the Calabrian arc. Presently, seismic swarms are active in the gap area, creating concerns for possible future large earthquakes. In this study, we model the deep Earth structure across the Pollino range to give new insights on the kinematics and tectonics of this enigmatic area. Migrated receiver function profiles show a subvertical lithospheric discontinuity, delineated by an abrupt change in Moho depth and mantle fabrics across the range. The lithospheric-scale discontinuity bounds the area of earthquake swarm activity and likely decouples the delamination-related extension of the Apennines from the extensional collapse of the Calabrian fore arc. This large-scale discontinuity implies that the normal faults are segmented across the range, limiting the lateral extent of faults where future earthquakes might occur.

1. Introduction

At the beginning of the past century, Omori Fusakichi recognized that large earthquakes in Italy align along the crest of the Apennines and identified two main seismic gaps, one in central Abruzzi and one in the Pollino area [*Omori*, 1909; see also *Valensise and Pantosti*, 2001]. Few years after the Omori observation, the M_s 6.9, 1915 Fucino earthquake struck the Abruzzi gap, while the 60 km long Pollino gap is still missing a large earthquake [*Cinti et al*., 2002]. While seismicity remained almost absent during several decades within the seismic gap (Figure 1), seismic swarm activity started in 2010, which has raised concerns of a future large earthquake. During this long swarm [*Totaro et al*., 2013], seismicity remains confined close to the Pollino mountain range, culminating with a M_w5.2 event on 25 October 2012 (Figure 1b).

The seismic gap is located at the hinge between the southern Apennines and the Calabrian arc (Figure 1), where the belt-parallel normal faults rotate from NW to N-S trending. The impact for seismic hazard evaluation is significant, because of the uncertainties on geometry and length of active faults, as well as rupture mechanisms. Paleoseismological trenches across normal faults at the southern border of the Pollino range [*Cinti et al*., 2002; *Michetti et al*., 1997] reported evidences for some paleo-earthquakes, the youngest of which occurred before 1 ka. Vertical slip rates of about 1 mm/yr found by trench studies [*Cinti et al*., 2002] are consistent with those estimated by GPS data [*D'Agostino et al*., 2011], suggesting that the extension tectonics remains almost stationary over the Holocene. Recent studies evidenced that the area is still affected by the evolution of the Calabrian arc [*Ferranti et al*., 2014; *Orecchio et al*., 2015].

This paper contributes by clarifying the tectonics of this key region, by imaging the crust/upper mantle structure across the Pollino range. High quality broadband data have been used to compute a *P* wave receiver function (RF) data set along profiles normal to the boundary between the Southern Apennines and the Calabrian arc and perpendicular to the Ionian subduction. RFs are migrated at depth along the profiles following the approach in *Bianchi et al*. [2010] and *Piana Agostinetti et al*. [2011] to highlight and enhance the continuity of the deep seismic structure. The recovered lithospheric structure helps constrain tectonic and kinematic models, which can improve our understanding of seismic hazard scenarios.

2. Data and Methods

P wave RFs are time series of *P*-to-*S* converted phases from teleseismic *P* wave [*Langston*, 1979]. *P* RFs are used worldwide for imaging the subsurface seismic structure at different depth-scales, from the shallow crust [e.g., *Leahy et al*., 2012; *Piana Agostinetti and Chiarabba*, 2008] to the Moho [e.g., *Licciardi et al*., 2014] and the upper mantle [*Piana Agostinetti and Miller*, 2014]. In this study, we used teleseismic data from about 80 broadband

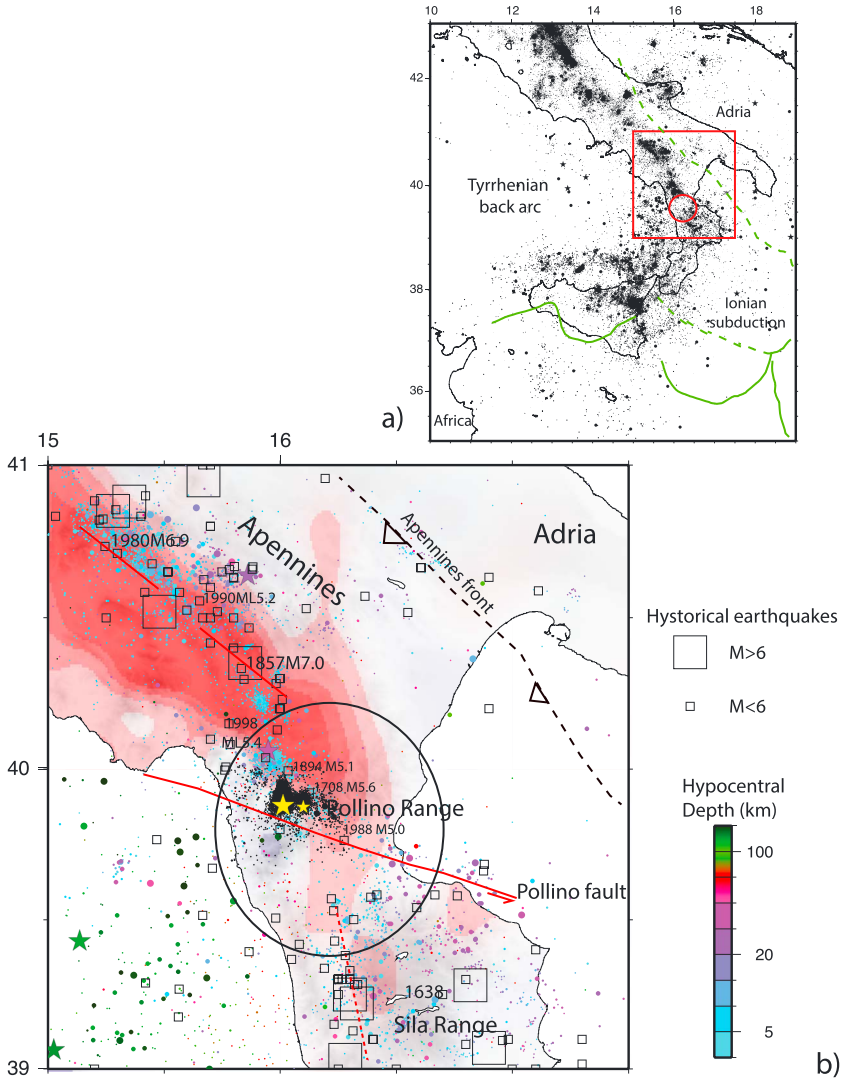

Figure 1. (a) Map of the past 30 years of instrumental seismicity in the southern Apennines and Tyrrhenian area [*Chiarabba et al*., 2014b]. The Pollino seismic gap is circled. (b) Zoom on the Pollino seismic gap area showing instrumental seismicity, the 2012 seismic swarm (black dots) and $M > 4$ earthquakes (yellow stars), the historical earthquakes (squares) from *Rovida et al*. [2011], and the low velocity (red anomaly) of the mantle [*Di Stefano et al*., 2009].

stations that belong to both permanent (Italian seismic Network, INGV) and temporary seismic networks operating in the area during the last decade [e.g., CATSCAN, *Steckler et al*., 2008]. Teleseismic data were selected after a visual inspection of only high S/N ratio *P* waves arrivals to discard noisy RF, obtaining an average of 50 high S/N ratio RF for each station. RF is computed using a frequency domain deconvolution [*Di Bona*, 1998], with a Gaussian filter with $a = 2$, i.e., with a cut-off frequency of about 1 Hz. The broad back azimuthal coverage obtained allowed to apply angular harmonic decomposition on the RF data set to separate the "constant" (or $k = 0$) contribution, i.e., the amplitudes in the RF time series which are independent from the back azimuth of the incoming *P* wave, from the higher harmonics ($k = 1,2$) which represents the periodicity of the amplitudes of the RF time series as a function of the back azimuth [*Farra and Vinnik*, 2000; *Schulte-Pelkum and Mahan*, 2014]. The constant component, or isotropic component, is related to the energy converted at velocity discontinuity between two isotropic layers, while the higher-order harmonics $k = 1,2$ represent the energy converted at a discontinuity between anisotropic layers, or dipping seismic interfaces [*Bianchi et al*., 2008]. This study analyses the first harmonics, $k = 0$, to highlight the discontinuities in the bulk velocity structure (i.e., isotropic structure). Using $k = 0$ harmonics has been proven to be superior to the simple analysis of stacked RF, and it has been used as input to RF inversion [e.g., *Shen et al*., 2013; *Amato et al*., 2014] and for interpretation of RF data set [*Chiarabba et al*., 2014a].

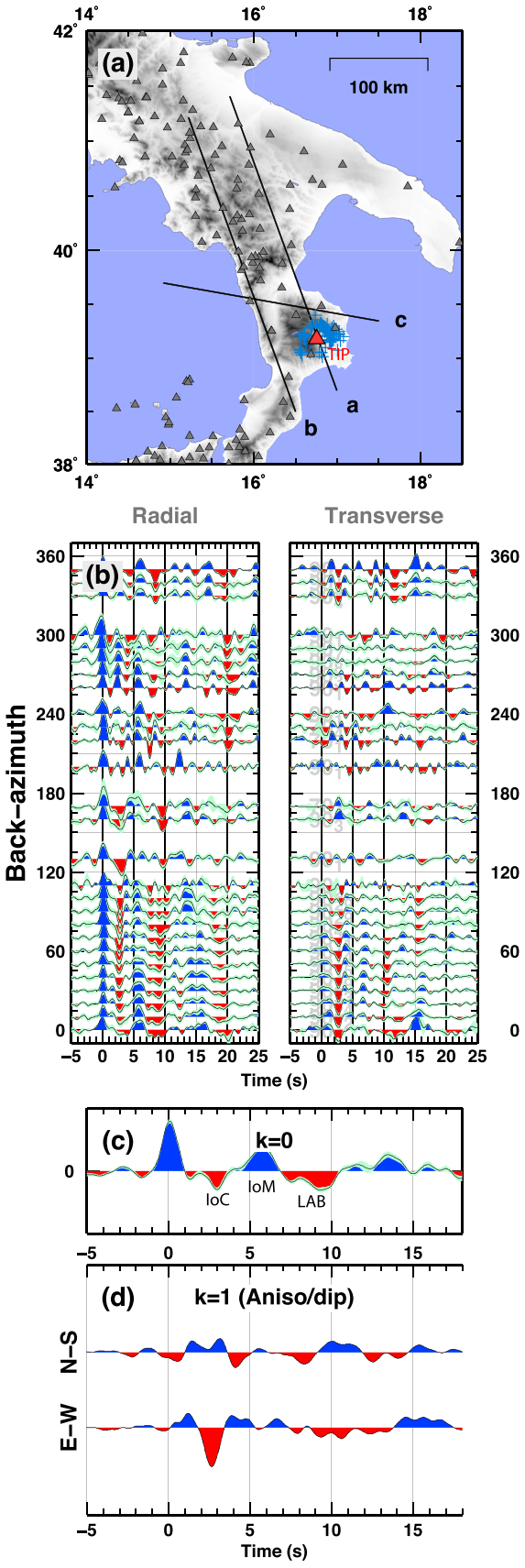

The analysis of the $k = 1,2$ harmonics could give insight into the presence of anisotropic materials at depth, but it is beyond the scope of the present study. The RFs have been stacked with harmonic weighting in the frequency domain.

Figure 2 shows the analysis for station TIP, situated on top of the Sila range. The distribution of the piercing points at 40 km depth of the teleseismic waves used for the computation of the RF data set displays almost complete back azimuth coverage. Teleseismic *P* waves sample the Ionian subduction zone where the crust of the overriding plate and the Ionian crust are still coupled [*Minelli and Faccenna*, 2010]. In Figure 2b, the back azimuthal (baz) sweep of the RF data set is shown. Blue (red) pulses indicate positive (negative) amplitudes related, on the radial RF data set, to the presence of positive (negative) velocity jumps. The Radial component of the RF data set displays positive arrivals at 5–6 and 14–16 s from all baz directions, while a negative arrival at about 2–4 s from N0 to 90E baz directions becomes positive between N240 and 340E. The presence of periodic pulses in the same time window is also evident from the analysis of the Transverse component of the RF data set. To separate the constant component of the RF data set from the periodic components, the RF data set is decomposed in angular harmonic coefficients. On the $k = 0$ harmonics (Figure 2c), which represents the *P* wave energy converted at a seismic discontinuity between two isotropic layers, positive pulses at about 5–6 and 14 s, already found in the baz sweep, are observed together with an elusive negative pulse at about 3 s,

Figure 2. (a) Location of the seismic station TIP (red triangle). Blue crosses indicate the surface projection of the piercing points of the teleseismic *P* wave analyzed, at 40 km depth. Grey triangles show the position of the seismic stations analyzed in this study. Black lines are the traces of the profiles reported in Figure 3. (b) RF data set for station TIP as a function of the back azimuth of the incoming *P* wave. Blue (red) pulses indicate positive (negative) amplitudes. On the left (right), the Radial (Transverse) component of the RF data set is shown. (c) The $k = 0$ harmonic coefficient of the RF data set for station TIP. Energy on the first harmonics relates to velocity jumps at depth. IoM = Ionian Moho and IoC = Ionian crust. (d) The $k = 1$ harmonic coefficient of the RF data set for station TIP. The harmonics is decomposed along two perpendicular axes, North-South (top) and East-West (bottom). Energy on the $k = 1$ harmonics relates to anisotropy and/or dipping interfaces at depth.

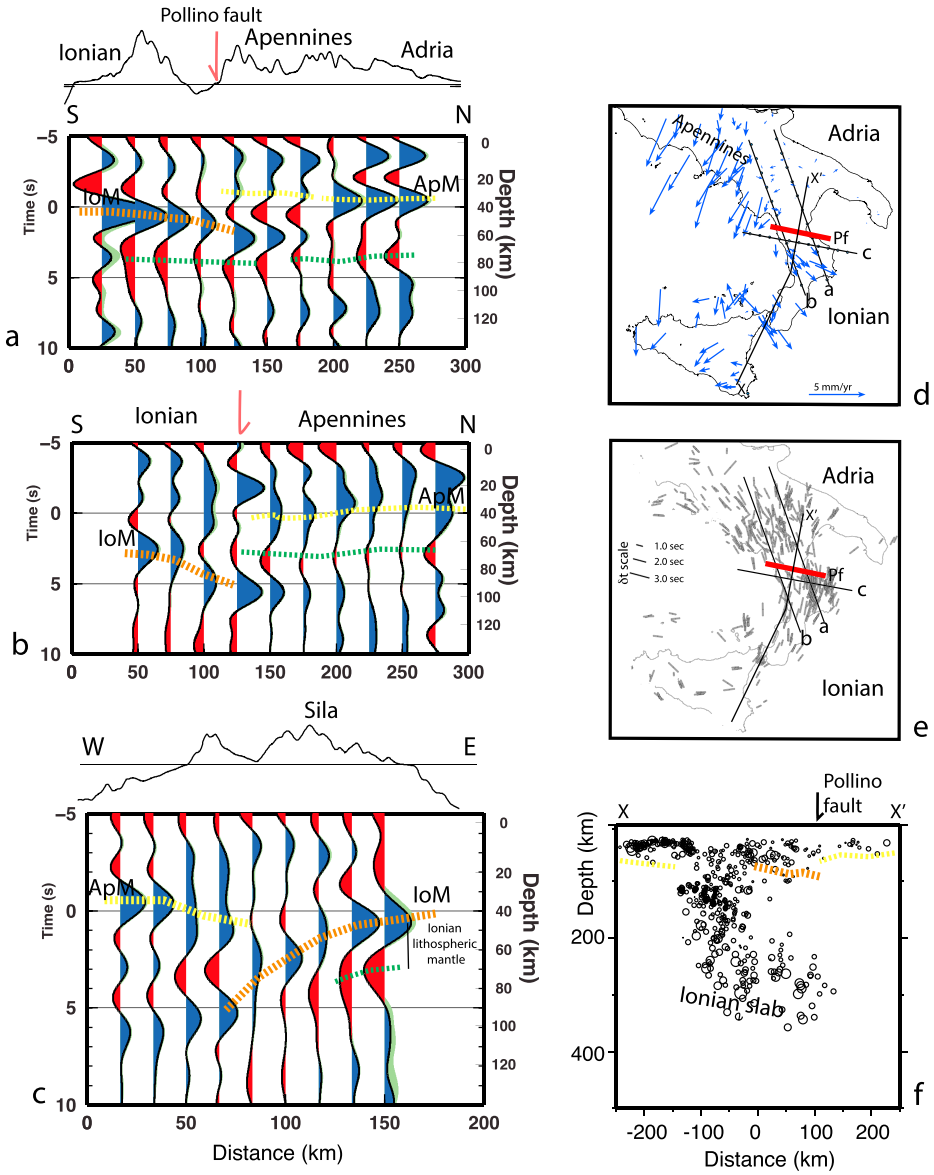

Figure 3. (a) RFs migrated profile across the Pollino range. Blue and red wiggles indicates the depth of positive and negative velocity contrasts, ApM = Apulian Moho, IoM = Ionian Moho, green dashed lines = LAB and (b) same as Figure 3a but crossing the range western limit; (c) RFs migrated profile across the Calabrian arc, showing the Tyrrhenian-dipping Ionian lithosphere, note the reduced thickness of the mantle lithosphere; (d) GPS velocity in a Apulian fixed framework, taken from *D'Agostino et al.* [2011]. Note the different velocities across the Pollino fault; (e) SKS anisotropy of the mantle taken from *Baccheschi et al.* [2011]; Note the different fabric across the Pollino fault; (f) Hypocenter of deep earthquakes with the courtesy of Pasquale De Gori.

which was not clear in Figure 2b. Such pulse is related to the top of the subducted Ionian crust and sediments (IoC) [*Piana Agostinetti et al.*, 2009]. A broad negative arrival is found at about 7–10 s, likely associated with the negative velocity jump at the Ionian Lithosphere-Asthenosphere boundary (LAB).

To improve imaging of the isotropic component and focusing on the Moho geometry, RFs are migrated at 40 km depth, by using the common conversion point (CCP) approach [*Bianchi et al.*, 2010]. Each of the three computed profiles has been sampled every 25 km; i.e., assuming a "spot" point every 25 km along the profile. RFs from different stations are associated to a spot if their piercing points at 40 km depth fall in a 25×50 km box centered on the spot. EW profile across the Sila range is sampled every 16 km, with 16×100 km boxes. Finally, angular harmonic decomposition is applied to all the RF belonging to each spot. It is important to notice that the CCP approach helps to suppress multiples from local-scale, shallow intracrustal discontinuities.

3. Results and Interpretations

Figure 3 shows the "isotropic" component of the RF data set projected along three profiles: profiles "a" and "b" across the Pollino range and profile "c" across the Ionian subduction system. Dots along the profiles in Figure 3d indicate the points where we apply CCP stacking for the reconstruction of the subsurface structures. Following the convention adopted in the previous section, blue and red pulses indicate positive and negative *S* wave velocity contrasts. The main positive contrast down to the upper mantle is the Moho conversion and the main negative pulse below the Moho is usually associated with the LAB [*Rychert and Shearer*, 2009].

Along the Apulian foreland (profile a, Figure 3a), a positive pulse at about 30 km depth can be ascribed to the *Ps* phase from the Moho [*Piana Agostinetti and Amato*, 2009; *Amato et al*., 2014]. The amplitude of such pulse decreases toward southeast, as seen also in *Steckler et al*. [2008] and *Piana Agostinetti et al*. [2008]. A positive pulse at the Southern termination of the same profile can be associated to the Ionian Moho [*Piana Agostinetti et al*., 2009]. The Moho pulse displays a discontinuity at about 125 km along the profile, where the pulse associated to the Ionian Moho seems to gently dip toward North (as previously noted in *Piana Agostinetti et al*. [2009]), leaving a 20 km of vertical offset between the Apulian Moho and the Ionian Moho. These observations are confirmed looking to profile b (Figure 3b), which runs parallel to profile a closer to the Tyrrhenian Sea. The continuity of the Moho pulse is interrupted at about 100 km along profile b, where due to a steeper dip of the Ionian Moho with respect to profile a, the vertical offset between the two Moho seems to be about 50 km.

A negative pulse arriving few seconds later than the Moho *Ps* is associated to the converted phases form the LAB. Remarkably, the depth of the LAB along profile remains almost constant under the entire profile a, without presenting any first-order discontinuity. The measures of LAB depth under the Apulian foreland are in agreement with results from *S*-RF analysis [*Miller and Piana Agostinetti*, 2012]. The negative pulses are less pronounced and vanish at about 100 km along profile b. In this case, there is no continuity of the LAB along the entire profile.

Along profile c, the CCP image depicts the main seismic structures of the Ionian subduction zone. A west dipping positive pulse under Mount Sila deepening from 40 to 80 km depth, defines the subducting Ionian Moho (IoM) in agreement with observations by *Piana Agostinetti et al*. [2009]. A broad NW dipping negative pulse is visible at the eastern end of the profile. This pulse represents *Ps* converted phases from the LAB. Thickness of the Ionian lithospheric mantle between the two discontinuities is as small as 30 km. At the other end of profile c, a sharp positive pulse can be followed at about 40–50 km depth before terminating at about 75 km along the profile. This pulse is interpreted as the marker of the Apulian Moho (ApM) flexed under the Apennines.

4. Discussion

The Pollino seismic gap is a great dilemma of the central Mediterranean geodynamic puzzle. Its location at the hinge between two blocks with different evolution during the Plio-Pleistocene might suggest that the absence of large earthquakes is at least partially controlled by lateral changes in deformation and discontinuity of processes along the mountain belt. On the other end, the continuous belt tectonic model proposed by *Valensise and Pantosti* [2001], based on the sudden tectonics change occurred at 0.7 Myr coupled with the rapid uplift of Calabria [*Westaway*, 1993], suggests the existence of a 60 km long section of the extensional system, where a large earthquake is missing over the past 1–2 Kyr [see also *Cinti et al*., 2002].

Our results show a lateral change in the mantle structure outlining the existence of a lithospheric fault that bounds the Pollino range (Pollino fault in Figure 3b). This fault limits the southward extent of the low Vs sublithospheric mantle upraised beneath the Apennines belt (see Figure 1b) and northward the extent of deep earthquakes within the slab (Figure 3f). SKS splitting measurements show a change in mantle fabric across the Pollino range [*Baccheschi et al*., 2011] (Figure 3e), consistent with the lithospheric discontinuity playing a role in decoupling deformation and mantle flow between the two blocks. However, SKS observations do not support the presence of mature toroidal mantle flow at asthenospheric depth level, in agreement with the limited amount of tearing along the discontinuity found here, where the LAB is discontinuous along profile b, but not along profile a. Since the magnitude of the SKS splitting is proportional to the amount of retreat [*Faccenda and Capitanio*, 2012], the absence of a well-developed mantle fabric consistent with a toroidal flow suggests a young age for the Pollino fault, or a limited amount of retreat, with an offset between the two edges of the lithosphere of less than the lithospheric thickness itself.

Active kinematic indicators (Figure 3d) and seismologic data suggest that the Pollino fault is not only young but it is still active, with kinematic discontinuity between the blocks on the two sides of the fault [*D'Agostino et al*., 2011; *Palano et al*., 2012; *Orecchio et al*., 2015]. Morphologic evidence of recent deformation at the submarine junction of the two blocks has been attributed to activity of an oblique fault consistent with an active discontinuity [*Ferranti et al*., 2014]. Instrumental seismicity occurs on this submarine area in the Ionian offshore, as well as historical events. All these evidences support the idea that the fault still accommodates the differential motion originated by the Ionian slab retreat.

Following our results, we propose that the Pollino fault is a discontinuity of structure and kinematics that segments the 60 km long gap. The active faults trenched until now, i.e., the Pollino range bounding faults [*Michetti et al*., 1997] and the Castrovillari fault [*Cinti et al*., 2002] are located northward of the lithospheric discontinuity on segments of faults at the very edge of the Apennines system.

South of the fault, the dominant process is the subduction of the Ionian lithosphere [*Chiarabba et al*., 2008, 2014b], which trace is well defined in RFs profiles (Figure 3c). Considering 20 km of accreted Calabrian wedge, the signal associated to the LAB suggests an oceanic lithosphere thickness of about 60 km, which is definitely smaller than the lithosphere thickness predicted from the classical thermal cooling model (about 100 km) [*Turcotte and Oxburgh*, 1967], but also it defines a thinner oceanic lithosphere than expected from a grain-boundary sliding model (about 70 km) [*Karato et al*., 2015; *Olugboji et al*., 2013]. The ultrathinned mantle lithosphere, observed in our study, points to an extreme erosion of the Ionian lithosphere, mechanism already proposed for the Apulian margin of the Ionian slab [*Miller and Piana Agostinetti*, 2011]. Our results indicate that this process of erosion is not limited to the continental margin but spread to the subducted Ionian lithosphere. The subduction of the ultrathinned lithosphere could be the cause for the gravitational collapse of the fore arc [*D'Agostino et al*., 2011] and recent stalling of the Ionian subduction with uplift of the Calabrian arc.

5. Conclusions

The lithospheric discontinuity identified in our study points to a decoupling of deformation across the Pollino range, from delamination controlled in southern Apennines to retreat controlled in the Calabrian fore arc. Lateral change in lithospheric structure revealed by RFs, seismicity, SKS anisotropy, GPS velocities, and recent deformation support the idea that the lithospheric fault is young and active and accommodate the differential retreat of the Ionian slab.

The 60 km long Pollino seismic gap is therefore segmented, with length and kinematics of faults in the area different from previously thought. This could impact on the definition of seismic hazard, whose application in medium to short term scenarios is actualized by the presence of seismic swarms.

Acknowledgments
We thank Jeff Park and an anonymous reviewer for their thoughtful comments on our manuscript. Data used in this study can be downloaded at the European waveform database: eida.rm.ingv.it. NPA research was research conducted with the financial support of Science Foundation Ireland & the Marie-Curie Action COFUND under Grant Number 11/SIRG/E2174.

References

Amato, A., I. Bianchi, and N. Piana Agostinetti (2014), Apulian crust: Top to bottom, *J. Geodyn*., *82*, 125–137, doi:10.1016/j.jog.2014.09.007.

Baccheschi, P., L. Margheriti, M. Steckler and E. Boschi (2011), Anisotropy patterns in the subducting lithosphere and in the mantle wedge: A case study – The Southern Italy subduction system, *J. Geophys. Res.*, *116*, B08306, doi:10.1029/2010JB007961.

Bianchi, I., N. Piana Agostinetti, P. De Gori, and C. Chiarabba (2008), Deep structure of the Colli Albani volcanic district (central Italy) from receiver functions analysis, *J. Geophys. Res.*, *113*, B09313, doi:10.1029/2007JB005548.

Bianchi, I., J. J. Park, N. Piana Agostinetti, and V. Levin (2010), Mapping seismic anisotropy using harmonic decomposition of receiver functions: An application to Northern Apennines, Italy, *J. Geophys. Res.*, *115*, B12317, doi:10.1029/2009JB007061.

Chiarabba, C., P. De Gori, and F. Speranza (2008), The southern Tyrrhenian subduction zone: Deep geometry, magmatism and Plio-Pleistocene evolution, *Earth Planet. Sci. Lett.*, *268*(3–4), 408–423.

Chiarabba, C., G. Giacomuzzi, I. Bianchi, N. P. Agostinetti, and J. Park (2014a), From underplating to delamination-retreat in the northern Apennines, *Earth Planet. Sci. Lett.*, *403*, 108–116, doi:10.1016/j.epsl.2014.06.041.

Chiarabba, C., P. De Gori, and F. Mele (2014b), Recent seismicity of Italy: Active tectonics of the central Mediterranean region and seismicity rate changes after the Mw 6.3 L'Aquila earthquake, *Tectonophysics*, doi:10.1016/j.tecto.2014.10.016.

Cinti, F., M. Moro, D. Pantosti, L. Cucci, and G. D'Addezio (2002), New constraints on the seismic history of the Castrovillari fault in the Pollino gap (Calabria, southern Italy), *J. Seismol.*, *6*, 199–217.

D'Agostino, N., E. D'Anastasio, A. Gervasi, I. Guerra, M. R. Nedimović, L. Seeber, and M. Steckler (2011), Forearc extension and slow rollback of the Calabrian Arc from GPS measurements, *Geophys. Res. Lett.*, *38*, L17304, doi:10.1029/2011GL048270.

Di Bona, M. (1998), Variance estimate in frequency-domain deconvolution for teleseismic receiver function computation, *Geophys. J. Int.*, *134*, 634–646, doi:10.1111/j.1365-246X.1998.00523.x.

Di Stefano, R., E. Kissling, C. Chiarabba, A. Amato, and D. Giardini (2009), Shallow subduction beneath Italy: Three-dimensional images of the Adriatic-European-Tyrrhenian lithosphere system based on high-quality *P* wave arrival times, *J. Geophys. Res.*, *114*, B05305, doi:10.1029/2008JB005641.

Faccenda, M., and F. A. Capitanio (2012), Development of mantle seismic anisotropy during subduction-induced 3-D flow, *Geophys. Res. Lett.*, *39*, L11305, doi:10.1029/2012GL051988.
Farra, V., and L. P. Vinnik (2000), Upper mantle stratification by P and S receiver functions, *Geophys. J. Int.*, *41*, 699–712.
Ferranti, L., P. Burrato, F. Pepe, E. Santoro, M. E. Mazzella, D. Morelli, S. Passaro, and G. Vannucci (2014), An active oblique-contractional belt at the transition between the Southern Apennines and Calabrian Arc: The Amendolara Ridge, Ionian Sea, Italy, *Tectonics*, *33*, 2169–2194, doi:10.1002/2014TC003624.
Karato, S., T. Olugboji, and J. Park (2015), Mechanisms and geologic significance of the mid-lithosphere discontinuity in the continents, *Nat. Geosci.*, *8*, 509–514, doi:10.1038/ngeo2462.
Langston, C. A. (1979), Structure under Mount Rainier, Washington, inferred from teleseismic body waves, *J. Geophys. Res.*, *84*, 4749–4762, doi:10.1029/JB084iB09p04749.
Leahy, G. M., R. L. Saltzer, and J. Schmedes (2012), Imaging the shallow crust with teleseismic receiver functions, *Geophys. J. Int.*, *191*, 627–636, doi:10.1111/j.1365-246X.2012.05615.x.
Licciardi, A., N. Piana Agostinetti, S. Lebedev, A. J. Schaeffer, P. W. Readman, and C. Horan (2014), Moho depth and Vp/Vs in Ireland from teleseismic receiver functions analysis, *Geophys. J. Int.*, *199*, 561–579, doi:10.1093/gji/ggu277.
Michetti, A. M., L. Ferreli, L. Serva, and E. Vittori (1997), Geological evidence for strong historical earthquakes in an 'aseismic' region: The Pollino case, *J. Geodyn.*, *24*(1–4), 67–86.
Miller, M., and N. Piana Agostinetti (2011), Erosion of the continental lithosphere at the cusps of the Calabrian arc: Evidence from S receiver functions analysis, *Geophys. Res. Lett.*, *38*, L23301, doi:10.1029/2011GL049455.
Miller, M., and N. Piana Agostinetti (2012), Insights into the evolution of the Italian lithospheric structure from S receiver function analysis, *Earth Planet. Sci. Lett.*, *345–348*, 49–59.
Minelli, L., and C. Faccenna (2010), Evolution of the Calabrian accretionary wedge (central Mediterranean), *Tectonics*, *29*, TC4004, doi:10.1029/2009TC002562.
Olugboji, T. M., S. Karato, and J. Park (2013), Structures of the oceanic lithosphere-asthenosphere boundary: Mineral-physics modeling and seismological signatures, *Geochem. Geophys. Geosyst.*, *14*, 880–901, doi:10.1002/ggge.20086.
Omori, F. (1909), Preliminary report on the Messina–Reggio Earthquake of Dec. 28, 1908, *Bull. Imp. Earth. Invest. Comm.*, *3*(2), 37–46.
Orecchio, B., D. Presti, C. Totaro, S. D'Amico, and G. Neri (2015), Investigating slab edge kinematics through seismological data: The northern boundary of the Ionian subduction system (south Italy), *J. Geodyn.*, *88*, 23, doi:10.1016/j.jog.2015.04.003.
Palano, M., L. Ferranti, C. Monaco, M. Mattia, M. Aloisi, V. Bruno, F. Cannavò, and G. Siligato (2012), GPS velocity and strain fields in Sicily and southern Calabria, Italy: Updated geodetic constraints on tectonic block interaction in the central Mediterranean, *J. Geophys. Res.*, *117*, B07401, doi:10.1029/2012JB009254.
Piana Agostinetti, N., and A. Amato (2009), Moho depth in peninsular Italy from teleseismic receiver functions, *J. Geophys. Res.*, *114*, B06303, doi:10.1029/2008JB005899.
Piana Agostinetti, N., and C. Chiarabba (2008), Seismic structure beneath Mt. Vesuvius from receiver function analysis and local earthquakes tomography: Evidences for location and geometry of the magma chamber, *Geophys. J. Int.*, *175*(3), 1298–1308, doi:10.1111/j.1365-246X.2008.03868.x.
Piana Agostinetti, N., and M. S. Miller (2014), The fate of the downgoing oceanic plate: Insight from the northern Cascadia subduction zone, *Earth Planet. Sci. Lett.*, *408*, 237–251, doi:10.1016/j.epsl.2014.10.016.
Piana Agostinetti, N., J. Park, and F. P. Lucente (2008), Mantle wedge anisotropy in Southern Tyrrhenian Subduction Zone (Italy), from receiver function analysis, *Tectonophysics*, *462*(1–4), 35–48, doi:10.1016/j.tecto.2008.03.020.
Piana Agostinetti, N., M. Steckler, and F. P. Lucente (2009), Imaging the subducted slab under the Calabrian Arc, Italy, from receiver function analysis, *Lithosphere*, *1*(3), 1–8, doi:10.1130/L49.1.
Piana Agostinetti, N., I. Bianchi, A. Amato, and C. Chiarabba (2011), Fluid migration in continental subduction: The Northern Apennines case study, *Earth Planet. Sci. Lett.*, *302*, 3–4, doi:10.1016/j.epsl.2010.10.039.
Rovida, A., R. Camassi, P. Gasperini, and M. Stucchi (Eds.) (2011), *CPTI11, the 2011 Version of the Parametric Catalogue of Italian Earthquakes*, Ist. Naz. di Geofis. e Vulcanol., Milan, Italy, doi:10.6092/INGV.IT-CPTI11.
Rychert, C. A., and P. M. Shearer (2009), A global view of the lithosphere asthenosphere boundary, *Science*, *324*(5926), 495–498, doi:10.1126/science.1169754.
Schulte-Pelkum, V., and K. H. Mahan (2014), A method for mapping crustal deformation and anisotropy with receiver functions and first results from USArray, *Earth Planet. Sci. Lett.*, *402*, 221–233.
Shen, W., M. H. Ritzwoller, V. Schulte-Pelkum, and F.-C. Lin (2013), Joint inversion of surface wave dispersion and receiver functions: A Bayesian Monte-Carlo approach, *Geophys. J. Int.*, *192*, 807–836, doi:10.1093/gji/ggs050.
Steckler, M. S., N. Piana Agostinetti, C. K. Wilson, P. Roselli, L. Seeber, A. Amato, and A. Lerner-Lam (2008), Illumination of the crustal structure in the Southern Apennines using teleseismic receiver functions, *Geology*, *36*(2), 155–158.
Totaro, C., D. Presti, A. Billi, A. Gervasi, B. Orecchio, I. Guerra, and G. Neri (2013), The Ongoing Seismic Sequence at the Pollino Mountains, Italy, *Seismol. Res. Lett.*, *84*, doi:10.1785/0220120194.
Turcotte, D. L., and E. R. Oxburgh (1967), Finite amplitude convection cells and continental drift, *J. Fluid Mech.*, *28*, 29–42.
Valensise, G., and D. Pantosti (2001), Seismogenic faulting, moment release patterns and seismic hazard along the central and southern Apennines and the Calabrian Arc, in *Anatomy of an Orogen: The Apennines and Adjacent Mediterranean Basins*, edited by G. B. Vai and I. P. Martini, pp. 495–512, Kluwer Acad., Dordrecht, Netherlands.
Westaway, R. (1993), Quaternary uplift of southern Italy, *J. Geophys. Res.*, *98*, 21,741–21,772, doi:10.1029/93JB01566.